International Journal of Automotive Technology, Vol. 6, No. 5, pp. 529–536 (2005)

Copyright © 2005 KSAE
1229-9138/2005/023-13

FUZZY TORQUE CONTROL STRATEGY FOR PARALLEL HYBRID ELECTRIC VEHICLES

J.-H. PU*, C.-L. YIN and J.-W. ZHANG

Institute of Automotive Engineering, Shanghai Jiao Tong University, Shanghai 200030, China

(Received 3 August 2004; Revised 10 May 2005)

ABSTRACT–This paper presents a novel design of a fuzzy control strategy (FCS) based on torque distribution for parallel hybrid electric vehicles (HEVs). An empirical load-regulating vehicle operation strategy is developed on the basis of analysis of the components efficiency map data and the overall energy conversion efficiency. The aim of the strategy is to optimize the fuel economy and balance the battery state-of-charge (SOC), while satisfying the vehicle performance and drivability requirements. In order to accomplish this strategy, a fuzzy inference engine with a rule-base extracted from the empirical strategy is designed, which works as the kernel of a fuzzy torque distribution controller to determine the optimal distribution of the driver torque request between the engine and the motor. Simulation results reveal that compared with the conventional strategy which uses precise threshold parameters the proposed FCS improves fuel economy as well as maintains better battery SOC within its operation range.

KEY WORDS : Parallel hybrid electric vehicle, Control strategy, Fuzzy control, Torque distribution

1. INTRODUCTION

The function of the control strategy of a hybrid electric vehicle (HEV) is to manage the energy use and to control the powertrain operation. The performance of an HEV depends largely upon its control strategy that is the brain of the vehicle. The hybrid powertrain, which comprises the heat engine, electric motor, power battery, automatic clutch and transmission, etc., is a nonlinear dynamical integrated system of electrical, mechanical, chemical and thermodynamic devices. Synergetic operation between different components is so complicated that it is difficult to construct an accurate mathematical model of the hybrid powertrain. Therefore, conventional control system design based on control theory is not applicable.

Much research work addressed to the control strategy of parallel HEVs has been conducted in recent years. They can be roughly classified into four categories. The first type is logic switch control strategy that uses a set of control parameters to define operating windows for each power component in accordance to a fixed control logic (Ehsani *et al.*, 1999; Lin *et al.*, 2001; Wipke *et al.*, 1999). The second type is instantaneous optimization control strategy based on real-time computation of the equivalent fuel consumption and emissions at possible operating points (Johnson *et al.*, 2000; Paganelli *et al.*, 2000, 2001). The third type is intelligent control strategy using fuzzy logic or neural networks (Baumann *et al.*, 2000; Koo *et al.*, 1998; Lee *et al.*, 1998; Schouten *et al.*, 2002, 2003). The fourth type employs global optimization techniques such as dynamic programming (Lin *et al.*, 2003), mathematic programming (Galdi *et al.*, 2001) and optimization algorithms based on classical variational approach (Delprat *et al.*, 2002). Global optimization techniques are not implementable in real-time control because they require a priori known driving cycle. They are currently used as a benchmark based on which real-time control strategy can be improved or compared against. Heavy computational requirements also limit the application of instantaneous optimization strategy to real-time control. The basic ideas of the first and the third type of parallel HEV control strategy are similar: they are all rule-based. Rule-based method is still the most feasible in the design of HEV control strategy at present (Jalil *et al.*, 1997; Johnson *et al.*, 2000; Lin *et al.*, 2003). Fuzzy control is a sort of rule-based intelligent control technique (Passino and Yurkovich, 1998). Ohio State University and Oakland University, with the support from US PNGV Program, are among the few pioneers in doing research on application of fuzzy control in HEV (Baumann *et al.*, 2000; Schouten *et al.*, 2002). The first published usage of fuzzy logic in HEV control includes Koo *et al.* (1998) and Lee *et al.* (1998). These researches show the potential of fuzzy logic in controlling the hybrid power-

*Corresponding author. e-mail: pujh@sjtu.edu.cn

train of complexity, strong nonlinearity and uncertainty.

Inspired by these achievements, a novel design of a fuzzy control strategy for a parallel HEV is presented in this paper. It is based on torque distribution, which is consistent with the development of the torque control technique of engine (Gerhardt *et al.*, 1998). Advantages of the torque-control-based strategy include the ease in handling drivability control and the expandability for integrating vehicle dynamic control in the future. The remainder of this paper is organized as follows: Section 2 presents the development of the rule-based torque distribution control strategy, followed by the description of its implementation using fuzzy logic in Section 3; Simulation results are presented in Section 4; and Section 5 gives our conclusions.

2. TORQUE DISTRIBUTION CONTROL STRATEGY

The specific configuration of the powertrain of an existing prototype parallel HEV used in this study is given in Table 1 and Figure 1.

The basic operating modes of the hybrid powertrain are illustrated in Figure 2. The upper curve is the vehicle speed consisting of four driving patterns: starting up from stop (AC), driving at constant speed (CD), full accelerating (DE) and braking to a stop again (EF). This speed schedule indicates the six basic operating modes: (1) the vehicle starting up electrically and driven by the motor alone; (2) the ISG starting the engine quickly at point B;

Table 1. Basic vehicle parameters.

Engine	55 kW
Electric Motor	14 kW continuous, 21 kW peak
Power Battery	336VDC, 8Ah
Transmission	4-speed AMT
Vehicle Curb Weight	1400 kg

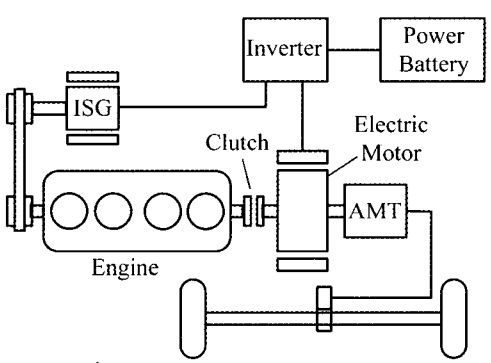

Figure 1. Powertrain configuration of the HEV.

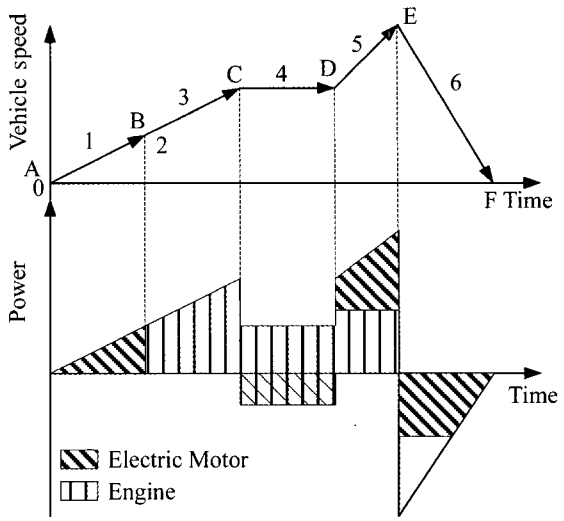

Figure 2. Typical driving schedule and the basic operating modes.

(3) the vehicle driven by the engine alone; (4) the engine driving the vehicle and driving the generator to charge the battery simultaneously; (5) the engine driving the vehicle with the motor assist in parallel at full acceleration; and (6) regenerative braking. The bottom curve in Figure 2 represents the driving power corresponding to the above speed schedule. Positive power is for acceleration and negative for deceleration.

The control strategy interprets the driver pedal motion as a torque request T_{req} being a function of the maximum torque available at the current vehicle speed. If $T_{req} < 0$, regenerative braking mode is activated and handled with a simple strategy: the motor recovers the maximum possible regeneration energy within constraints imposed by the motor and the battery. The deficiency of the brake torque, if exists, is made up by friction brakes. If $T_{req} \geq 0$, torque request is distributed between the engine and the motor as shown in Equation (1). The result of distribution determines the other operating modes of the powertrain.

$$T_{req} = T_e + T_m \tag{1}$$

The motor torque T_m in Equation (1), positive (motor assist) or negative (power generating), is used to regulate the load of the engine according to the efficiency map of the engine (Figure 3(a)). Figure 3(a) also presents the optimal efficiency curve T_{e_opt}, the maximum torque curve T_{e_max}, and the minimum operating torque curve T_{e_off}. The engine shuts off because of excessive inefficiency when the torque request falls below T_{e_off}.

Charging battery during driving by the engine-driven motor is defined as active charge. Charging battery by regenerative brake is defined as passive charge. The

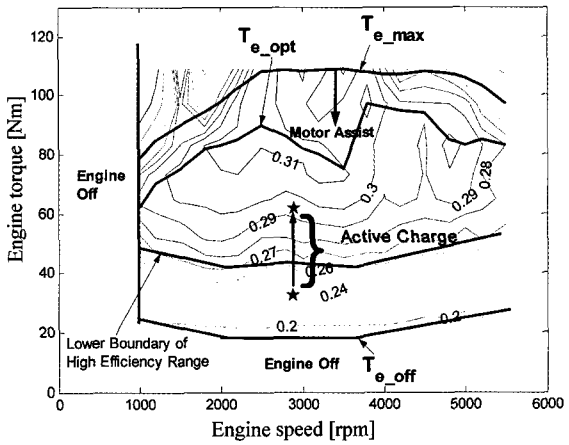

(a) Load regulation through active charge and motor assist

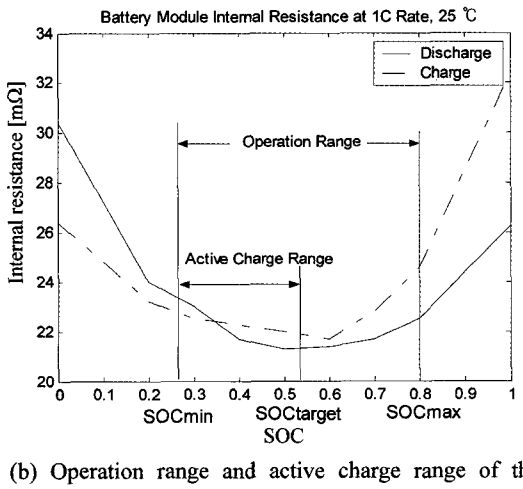

(b) Operation range and active charge range of the battery SOC

Figure 3. Rule-based control strategy.

engine is maintained operating in the high efficiency range by load regulation through active charge and motor assist. An advanced algorithm is used to maintain the battery state-of-charge (SOC) within its defined operation range, as shown in Figure 3(b), within which the internal resistances of both charge and discharge are relatively small and thus the battery losses are minimized. The lowest point of the internal resistance is marked as the target SOC. The active charge is more likely to happen when the SOC drops below the target while the discharge (motor assist or motor drive alone) is more likely to happen when the SOC rises above the target.

The T_{e_off} is determined by comparing the energy conversion efficiency of the engine driving the wheels directly with that of the motor driving. The energy conversion efficiency of the engine driving directly is computed as:

$$\eta_1 = \eta_e \eta_T \tag{2}$$

The energy conversion efficiency of the motor driving is computed as:

$$\eta_2 = \eta_e \eta_m \eta_{ess} \eta_m \eta_T \tag{3}$$

Where η_e is the engine efficiency, η_T is the transmission efficiency, η_m is the motor efficiency, and η_{ess} is the battery efficiency. The engine efficiency can be high in active charge in Equation (3). While in Equation (2), the engine efficiency may be low when the vehicle is propelled by the engine directly. When $\eta_1 \leq \eta_2$, the operating points of the engine are out of the high efficiency range. For example, when the efficiencies of the engine, the motor and the battery are 0.29, 0.86 and 0.9 respectively, the threshold of the efficiency for engine off will be 0.19, i.e., if the efficiency of the engine drops below 0.19, the engine will shut off. The corresponding torque of 0.19 is T_{e_off}. Unfortunately, it is much more complicated in the real world. Increment of fuel consumption resulting from load rise in active charge may be trivial due to the increase in efficiency. Moreover, passive charge does not consume fuel at all. Therefore, the T_{e_off} may be a little higher than the above value. Real-time analysis and comparison of the energy conversion efficiency are very difficult. A practical alternative is to determine the T_{e_off} and the high efficiency range of the engine with a couple of predefined threshold parameters as shown in Figure 3(a).

There are two gear shift strategies for engine on and off. The gear shift strategy optimizing the engine operation is chosen if the engine is on, and the one optimizing the motor operation (using the motor efficiency map) is chosen if the engine is off and the vehicle is driven electrically.

The above presented strategy can be formulated into a set of control rules in the form of IF...THEN... using Boolean logic computation to control the operating modes and the transitions between modes of the hybrid powertrain. This is the simple conventional rule-based logic threshold control strategy (LTCS) which uses precise threshold parameters. In real application, torque smooth control is necessary for modes transitions in order to achieve acceptable drivability (Tong *et al.*, 2003). A typical example is the transition from motor drive through engine start to engine drive. Smooth transition is realized by decreasing the motor torque gradually and increasing the engine torque gradually at the same time to maintain the equality between the driver torque request and the torque sum of the motor and the engine. In any situation, in order to get smooth torque transition, the fast-response motor torque is adjusted to the slow-response engine torque and affords necessary torque

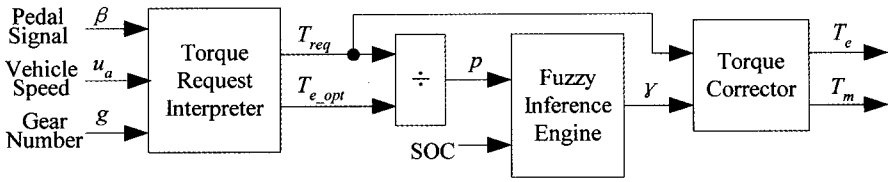

Figure 4. Block diagram of the fuzzy torque distribution controller.

compensation.

3. IMPLEMENTATION USING FUZZY LOGIC

Based on the rules developed above, a fuzzy control strategy (FCS) is developed by using fuzzy logic as a substitute for Boolean logic, and by using fuzzy parameters, such as "low", "medium" and "high", as substitutes for precise parameters. The FCS has finer rules than the LTCS because Boolean logic is binary-valued while fuzzy logic is multiple-valued.

The fuzzy torque distribution controller consisting of 3 modules is given in Figure 4. The first block interprets the driver pedal motion as a torque request and computes the T_{e_opt}. The second block is a fuzzy inference engine with two inputs: the ratio of the torque request to the T_{e_opt} and the battery SOC, and one output: normalized motor torque command with a universe of discourse [−1.5,1.5]. The third block computes the final values for the engine torque and the motor torque using Treq and γ. The motor torque is computed as:

$$T_m = \gamma T_{m\_\max} \tag{4}$$

Where $T_{m\_\max}$ is the motor maximum torque of continuous work under current speed. The engine torque is computed by Equation (1) with two exceptions: when $T_e < T_{e\_off}$, $T_e = 0$, $T_m = T_{req}$; when $T_e > T_{e\_\max}$, $T_e = T_{e\_\max}$.

The design of the inputs and output for the fuzzy inference engine is presented below. According to the efficiency map of the engine, torque requests are assigned 5 fuzzy values: (1) too low, the engine shuts off due to excessive low efficiency; (2) low, raise the engine load by active charge; (3) medium, the torque request is close to the optimal efficiency curve; (4) high, lower the engine load by motor assist; (5) too high, meeting the torque request has priority over saving fuel use. In order to exactly represent the strength of the torque request relative to the load rate of the engine, the ratio of the T_{req} to T_{e_opt} ($p = T_{req}/T_{e\_opt}$) is used to represent the torque request. Similarly, 5 fuzzy values are assigned to the battery SOC according to Figure 3(b). The universe of the output γ is partitioned into 7 primary fuzzy sets. Triangular and trapezoidal shapes, as shown in Figure 5, are selected for the membership functions of the inputs and output. Table 2 presents a list of control rules using the assignments of the inputs and output.

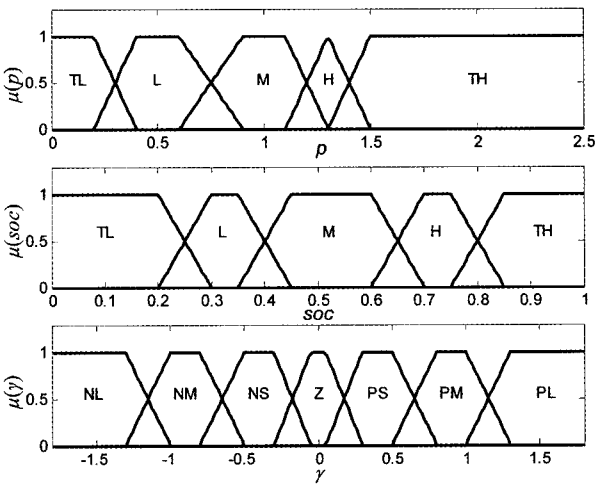

Figure 5. Membership functions for the inputs and output of the fuzzy inference engine. TL: Too Low, L: Low, M: Medium, H: High, TH: Too High, NL: Negative Large, NM: Negative Medium, NS: Negative Small, Z: Zero, PS: Positive Small, PM: Positive Medium, PL: Positive Large

Table 2. Rule-base of the fuzzy inference engine.

IF (p = = TL) AND (SOC = = ~TL) THEN γ = PS
IF (p = = TL) AND (SOC = = TL) THEN γ = NL
IF (p = = L) AND (SOC = = TL) THEN γ = NL
IF (p = = L) AND (SOC = = L) THEN γ = NS
IF (p = = L) AND (SOC = = M) THEN γ = NS
IF (p = = L) AND (SOC = = H) THEN γ = NS
IF (p = = L) AND (SOC = = TH) THEN γ = Z
IF (p = = M) AND (SOC = = TL) THEN γ = NS
…
…
IF (p = = TH) AND (SOC = = TH) THEN γ = PL

Let K is used to represent the total number of rules, and A_k, B_k, C_k the fuzzy values for inputs p, soc and output γ of the rule number k (k = 1, 2,..., K). The fuzzy inference process is described as follows:

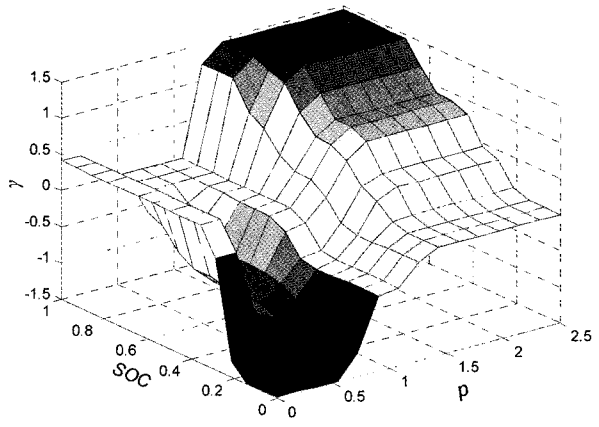

Figure 6. Output surface of the fuzzy inference engine.

1) Fuzzification: The membership degrees of the two fuzzy inputs, $\mu_{A_k}(p)$ and $\mu_{B_k}(soc)$, are computed using the membership functions of the inputs.
2) Rule matching: The degree of fulfillment for the antecedent of each rule (ρ_k) is computed using the fuzzy logic operators:
$\rho_k=\min(\mu_{A_k}(p), \mu_{B_k}(soc))$.
3) Inference: The fuzzy conclusion of an individual rule ($\mu^o_{C_k}(\gamma)$) is computed using the degree of fulfillment for the antecedent, the membership function of the consequent ($\mu_{C_k}(\gamma)$) and the implication operator:
$\mu^o_{C_k}(\gamma)=\rho_k\mu_{C_k}(\gamma)$.
4) Aggregation: All the fuzzy conclusions of individual rules are added up to an overall fuzzy output value:

$$\mu_C(\gamma)=\sum_{k=1}^{K}\mu^o_{C_k}(\gamma).$$

5) Defuzzification: Crisp output value (γ) is computed by applying the center of gravity (COG) defuzzification method to the fuzzy output:

$$\gamma=\frac{\int\gamma\mu_C(\gamma)d\gamma}{\int\mu_C(\gamma)d\gamma}=\frac{\sum_{k=1}^{K}d_k\int\mu^o_{C_k}(\gamma)d\gamma}{\sum_{k=1}^{K}\int\mu^o_{C_k}(\gamma)d\gamma}$$

where d_k is the center of gravity of $\mu^o_{C_k}(\gamma)$.

The above inference process can be easily programmed in computer language. Figure 6 presents the output surface of the fuzzy inference engine.

4. SIMULATION RESULTS

A forward-looking HEV simulation model developed at Shanghai Jiao Tong university (Pu *et al.*, 2004) is adopted to assess the performance of the FCS and the LTCS in comparison. This model is implemented in Simulink and verified with bench test data for an HEV prototype car. For more information of the model, the reader is referred to Pu *et al.* (2004). Simulation results for the two strategies using New European Driving Cycle (NEDC) are presented below.

Figure 7 presents the simulation results using the FCS

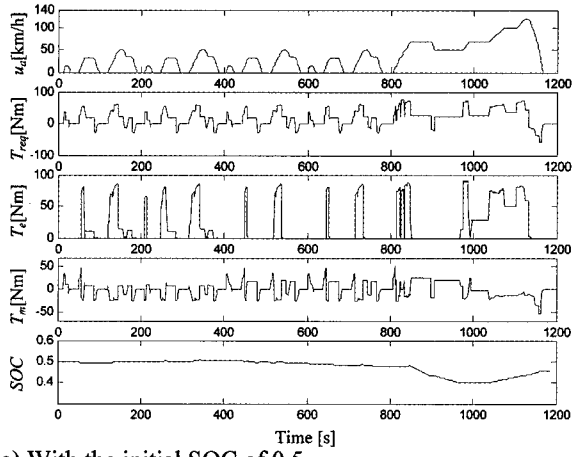

(a) With the initial SOC of 0.5

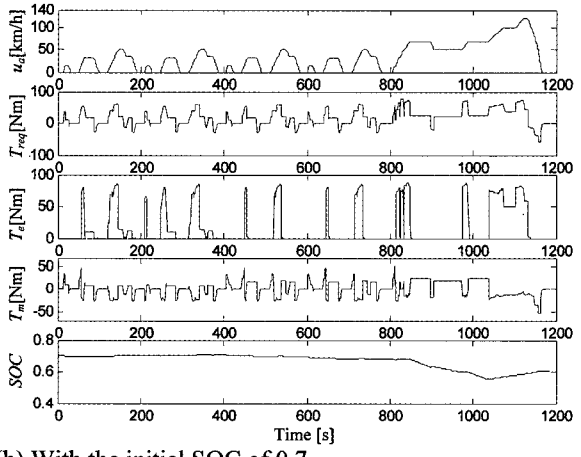

(b) With the initial SOC of 0.7

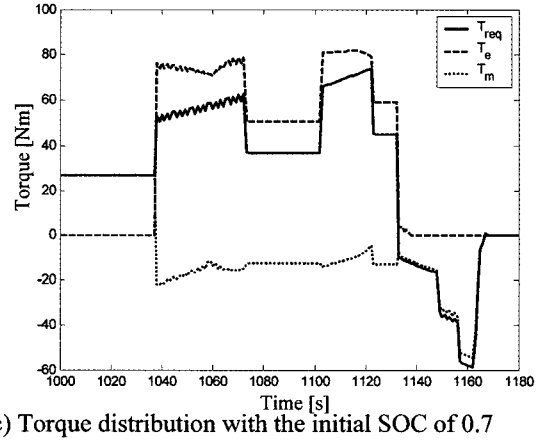

(c) Torque distribution with the initial SOC of 0.7

Figure 7. Simulation results using the FCS.

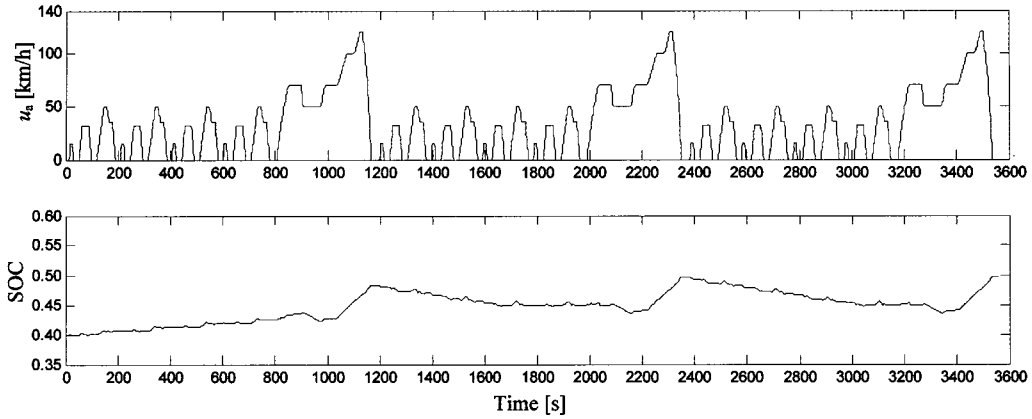

Figure 8. Change of the SOC over a long time horizon simulation. (a) With the initial SOC of 0.5 (b) With the initial SOC of 0.7

with the initial SOC of 0.5 and 0.7. Curves of the vehicle velocity (u_a), the torque request (T_{req}), the engine torque (T_e), the motor torque (T_m) and the battery SOC are presented in 7(a) and 7(b). Figure 7(c) gives the torque distribution plot of the last 200s in 7(b). Driving force is supplied by the motor alone between 1000–1180s when the torque request is small and the battery SOC is relatively high (0.62). With the vehicle acceleration and the torque request rise, the engine starts. The active charge is used to raise the engine load because the torque request is not high enough to make the engine operate at high efficiency. In the phase of deceleration, the motor supplies most of the brake force because of the small degree of brake. Figure 7 also reveals that the SOC remains within the operation range in spite of the initial SOC.

It can be observed more clearly that the FCS works very well in maintaining the SOC in Figure 8 which presents the change of the SOC over a long time horizon simulation (3 NEDCs). At the very beginning, the SOC is relatively low (0.4) and the FCS uses the engine heavily to recharge the battery in addition to meeting the vehicle demand. With the raise of the SOC, electricity usage increases. Lots of simulation results demonstrate the effectiveness of the FCS in maintaining the SOC.

Figure 9 presents the simulation results using the LTCS. It is observed from the comparison between Figure 9 and Figure 7 that, the engine torque is relatively uniform over the cycle in Figure 7, while relatively small in the city driving sector of low vehicle velocity in Figure 9. The engine probably frequently operates in non-high-efficiency range using the LTCS when the vehicle velocity is low.

For the purpose of investigating further the behavior of the engine, Figure 10 presents the engine operating points plotted on the efficiency map for the test with the initial

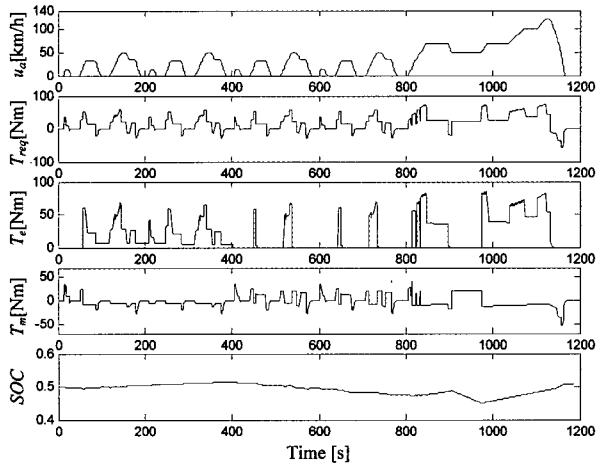

(a) With the initial SOC of 0.5

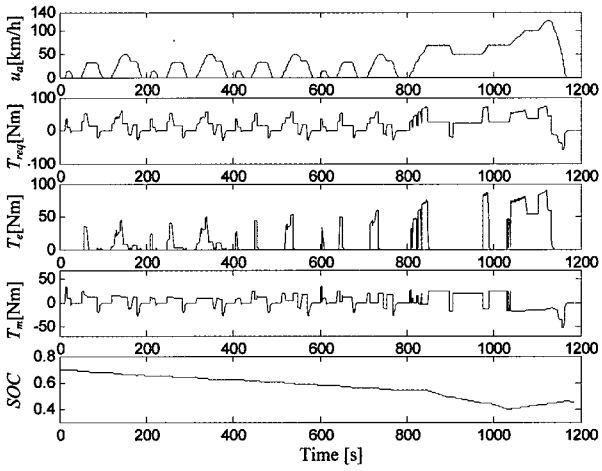

(b) With the initial SOC of 0.7

Figure 9. Simulation results using the LTCS.

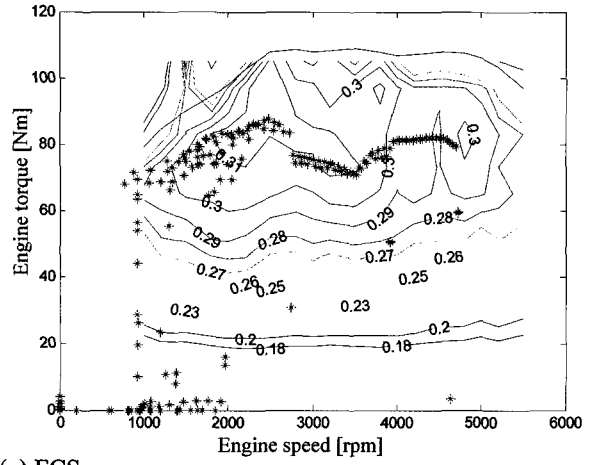

(a) FCS

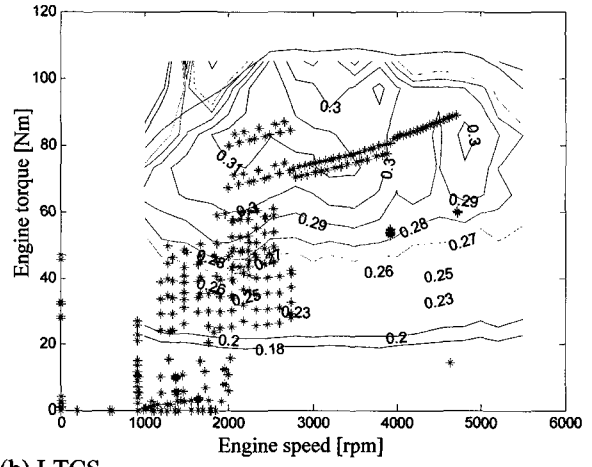

(b) LTCS

Figure 10. Operating points of the engine with the initial SOC of 0.7 using (a) the FCS; (b) the LTCS.

SOC of 0.7 for the two strategies. For the FCS the operating points of the engine are more concentrated in the high efficiency range, while for the LTCS the operating points of the engine are much more spread out over the map and many of them are in the low load and low efficiency range. This indicates that the FCS is more effective in controlling the engine operating in high efficiency range.

Table 3 presents the fuel economy of the vehicle and the efficiencies of the main components for the test with the initial SOC of 0.7. The data in Table 3 demonstrate again that the FCS is more effective than the LTCS in keeping the engine operating at high efficiencies. The average efficiency of the engine for the FCS is 23.95%, while that for the LTCS is only 18.69%. No significant difference exists between the average efficiencies of the two strategies for the motor and the battery, because the efficiencies of the motor and the battery are relatively high inherently, and the high efficiency ranges are much

Table 3. The fuel consumption of the vehicle and the efficiencies of the main components for the test with the initial SOC of 0.7.

Average efficiency	FCS	LTCS
Engine (%)	23.95	18.69
Motoring (%)	86.81	86.92
Generating (%)	82.43	79.99
Battery discharge (%)	93.13	93.73
Battery Charge (%)	87.43	87.82
Drivetrain (%)	81.37	81.17
Initial SOC (%)	70.00	70.00
End SOC (%)	61.00	50.00
Fuel economy (L/100 km)	6.27	6.00
Fuel economy with SOC correction (L/100 km)	6.62	7.24

wider and insensitive to load. Although the fuel economy for the LTCS (6 L/100 km) is less than that for the FCS (6.27 L/100 km), the SOC drops only by 9% for the FCS while by 20% for the LTCS. Seven sets of fuel economy and SOC change results are obtained by simulation over the same driving cycle seven times with different initial SOC from 0.4 to 0.7 for each run. A linear regression is used to calculate the corrected fuel economy corresponding to the zero SOC change over the cycle. The corrected fuel economy for the FCS is 6.62 L/100 km and for the LTCS is 7.24 L/100 km. It is thus obvious that the FCS is superior to the LTCS in terms of fuel economy.

5. CONCLUSION

This paper presents a systematic methodology for the development of a rule-based control strategy for a parallel HEV using fuzzy logic. Since it is difficult to construct an accurate mathematical model of the plant, rule-based method is still the most feasible in the design of HEV control strategy at present. Through studying the dynamics of the hybrid powertrain, empirical knowledge of how to best control the system is acquired and formulated into control rules. In respect of control knowledge formulation, fuzzy logic is superior to Boolean logic because fuzzy logic is much closer in spirit to human thinking and natural language. Therefore it can formulate the control strategy with finer rules and can achieve better control.

Comparative simulation is performed for the proposed strategy (FCS) and the conventional strategy using precise parameters (LTCS). It shows that the FCS improves fuel economy as well as maintains much better battery SOC within its operation range. Without heavy compu-

tation and independent of accurate mathematical model of the plant, the FCS has good real-time performance and robustness. Therefore, it is practical and suitable for application in real HEV.

ACKNOWLEDGEMENT–This work was supported by the Electric Vehicle Key Project of National 863 Program of China under contract No. 2001AA501200 and No. 2003AA501200.

REFERENCES

Baumann, B. M., Washington, G., Glenn, B. C. and Rizzoni, G. (2000). Mechatronic design and control of hybrid electric vehicles. *IEEE/ASME Trans. on Mechatronics* **5, 1,** 58–72.

Delprat, S., Guerra, T. M. and Rimaux, J. (2002). Control strategies for hybrid vehicles: optimal control. *Proc. the 56th IEEE Vehicular Technology Conference*, Vancouver, Canada, **3,** 1681–1685.

Ehsani, M., Gao, Y. and Butler, K. L. (1999). Application of electrically peaking hybrid (ELPH) propulsion system to a full-size passenger car with simulated design verification. *IEEE Trans. on Vehicular Technology* **48, 6,** 1779–1787.

Galdi, V., Ippolito, L., Piccolo, A. and Vaccaro, A. (2001). Multiobjective optimization for fuel economy and emissions of HEV using the goal-attainment method. *Proc. the 18th International Electric Vehicle Symposium*, Berlin, Germany.

Gerhardt, J., Honninger, H. and Bischof, H. (1998). A new approach to functional and software structure for engine management systems – BOSCH ME7. *SAE Paper No.* 98P–178(49).

Jalil, N., Kheir, N. A. and Salman, M. (1997). A rule-based energy management strategy for a series hybrid vehicle. *Proc. the American Control Conference*, Albuquerque, New Mexico, USA, 689–693.

Johnson, V. H., Wipke, K. B. and Rausen, D. J. (2000). HEV control strategy for real-time optimization of fuel economy and emissions. *SAE Paper No.* 2000-01-1543.

Kimura, A., Abe, T. and Sasaki, S. (1999). Drive force control of a parallel-series hybrid system. *JSAE Review* **20, 3,** 337–341.

Koo, E. S., Lee, H. D., Sul, S. K. and Kim J. S. (1998). Torque control strategy for a parallel-hybrid vehicle using fuzzy logic. *Proc. the 1998 IEEE Industry Applications Conference*, St.Louis, MO, USA, 1715–1720.

Lee, H. D., Sul, S. K. (1998). Fuzzy-logic-based torque control strategy for parallel-type hybrid electric vehicle. *IEEE Trans. on Industrial Electronics* **45, 4,** 625–632.

Lin, C. C., Filipi, Z., Wang, Y. *et al* (2001). Integrated, feed-forward hybrid electric vehicle simulation in Simulink and its use for power management studies. *SAE Paper No.* 2001-01-1334.

Lin, C. C., Peng, H., Grizzle, J. W. and Kang J.-M. (2003). Power management strategy for a parallel hybrid electric truck. *IEEE Trans. on Control Systems Technology* **11, 6,** 839–849.

Paganelli, G., Ercole, G., Brahma, A., Guezennec, Y. and Rizzoni, G. (2001). General supervisory control policy for the energy optimization of charge-sustaining hybrid electric vehicles. *JSAE Review* **22, 4,** 511–518.

Paganelli, G., Guerra, T. M., Delprat, S., Santin, J.-J., Delhom, M. and Combes, E. (2000). Simulation and assessment of power control strategies for a parallel hybrid car. *Proc. Institution Mechanical Engineers, Part D: J. Automobile Engineering* **214, 7,** 705–717.

Passino, K. M. and Yurkovich, S. (1998). *Fuzzy Control.* Addison-Wesley, Menlo Park, California.

Pu, J. H., Yin, C. L., Zhang, J. W. and Ma D. Z. (2004). Modeling and development of the control strategy for a hybrid car (in Chinese). *J. Shanghai Jiaotong University* **38, 11,** 1917–1921.

Schouten, N. J., Salman, M. A. and Kheir, N. A. (2002). Fuzzy logic control for parallel hybrid vehicles. *IEEE Trans. on Control Systems Technology* **10, 3,** 460–468.

Schouten, N. J., Salman, M. A. and Kheir, N. A. (2003). Energy management strategies for parallel hybrid vehicles using fuzzy logic. *Control Engineering Practice* **11, 2,** 171–177.

Tong, Y., Ouyang, M. and Zhang, J. (2003). Real-time simulation and research on control algorithm of parallel hybrid electric vehicle (in Chinese). *Chinese J. Mechanical Engineering* **39, 10,** 156–161.

Wipke, K. B., Cuddy, M. R. and Burch, S. D. (1999). ADVISOR 2.1: a user-friendly advanced powertrain simulation using a combined backward/forward approach. *IEEE Trans. on Vehicular Technology* **48, 6,** 1751–1761.